Supporting Information

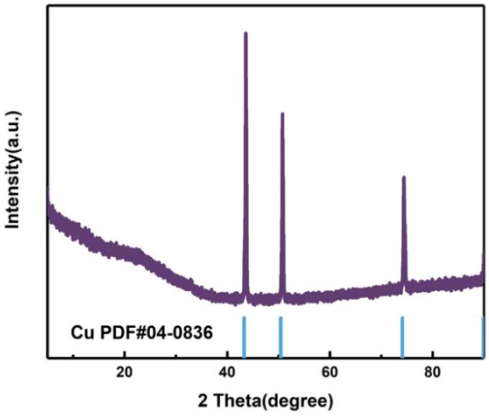

Figure S1 XRD pattern of NPCF.

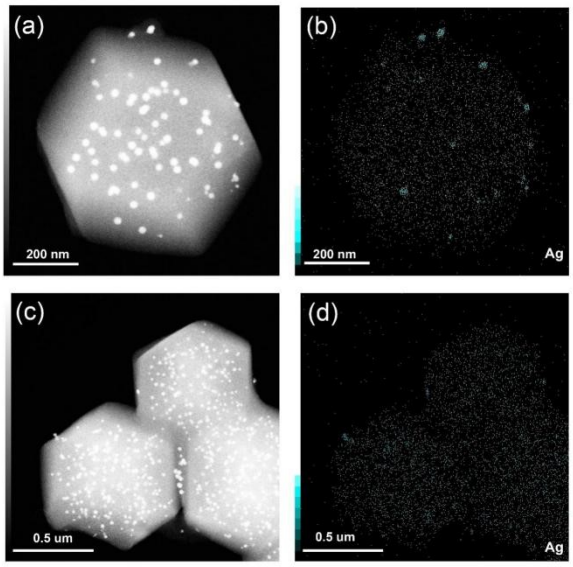

Figure S2 HRTEM of (a) (c)Ag NPs on the surface of Ag@NPCF and (b) (d) the corresponding elemental mapping of Ag.

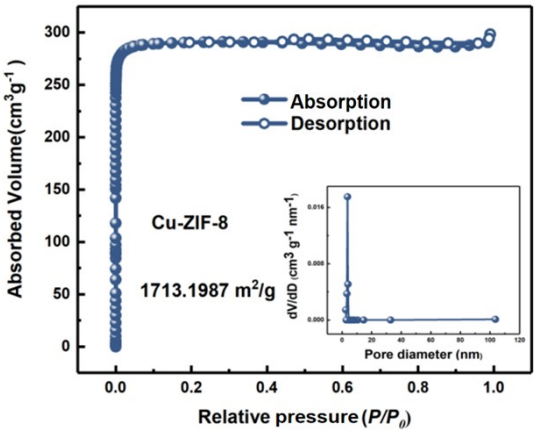

Figure S3 N_2 adsorption–desorption isotherm profiles of Cu-ZIF-8, and the corresponding pore size distribution in the inset.

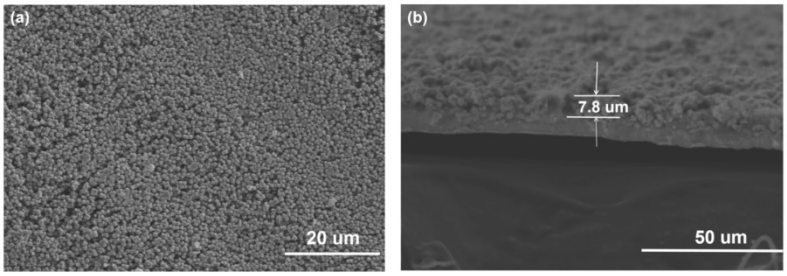

Figure S4 The top view (a) and cross-sectional view (b) of Ag@NPCF electrode.

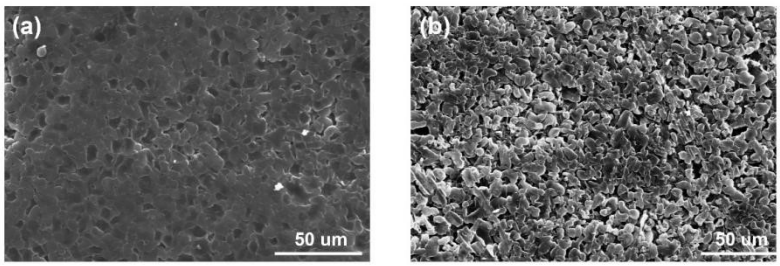

Figure S5 Top views of the (a) Ag@NPCF electrode and (b) pristine Cu foil electrode after 50 cycles at 0.5 mA cm^{-2} with a total capacity of 0.5 $mAh \cdot cm^{-2}$.

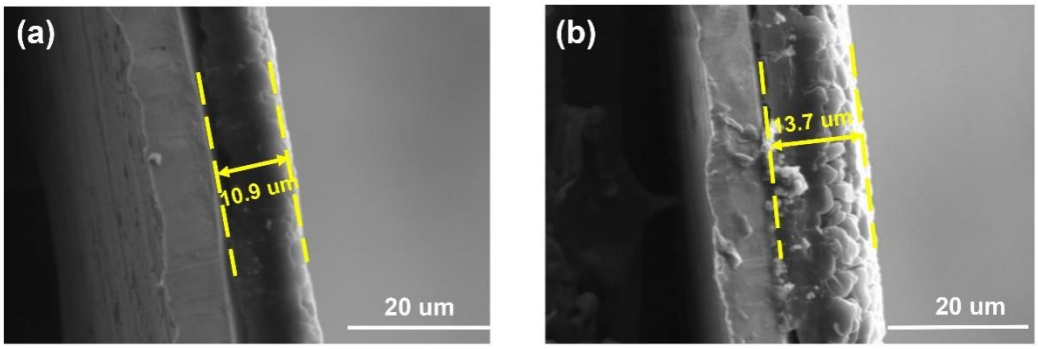

Figure S6 Cross-sectional views of the (a) Ag@NPCF electrode and (b) pristine Cu foil electrode after plating 2 $mAh \cdot cm^{-2}$ of Li at 0.5 $mA \cdot cm^{-2}$.

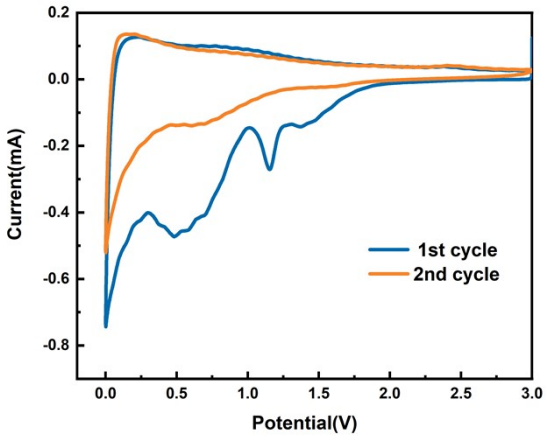

Figure S7 Cyclic voltammogram of NPCF electrode obtained at 0.1 mV s^{-1} in the potential window of 0.01–3.0 V.

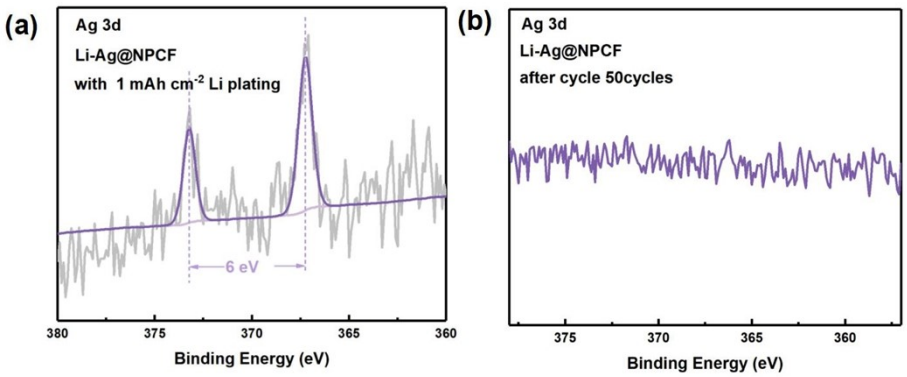

Figure S8 High-resolution XPS characterizations for Ag 3d. (a) Li-Ag@NPCF electrode (with 1 mAh cm^{-2} Li plating); (b) Li-Ag@NPCF electrodes (after cycle 50 cycles).

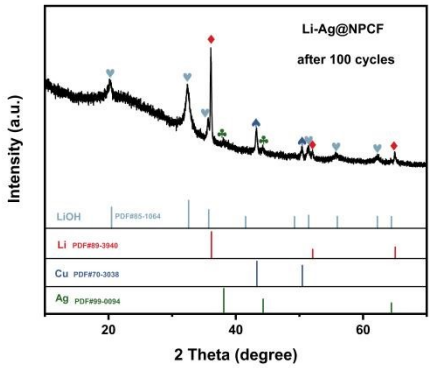

Figure S9 XRD image of Li-Ag@NPCF symmetric cells after 100 cycles

Electrodes		$R_s(\Omega)$	$R_{ct}(\Omega)$
Li-Cu	Before cycle	2.60	90.14
	After 50 cycles	2.37	34.51
Li-Ag@NPCF	Before cycle	3.57	58.33
	After 50 cycles	2.87	26.19

Table S1 Impedance parameters simulated from the equivalent circuits